Available online at www.sciencedirect.com
SCIENCE DIRECT®
Automatica 41 (2005) 1491–1502
automatica
www.elsevier.com/locate/automatica

Impulsively synchronizing chaotic systems with delay and applications to secure communication☆

A. Khadra[a,*], X.Z. Liu[a,1], X. Shen[b,1]

[a]Department of Applied Mathematics, University of Waterloo, Waterloo, Ont., Canada N2L 3G1
[b]Department of Electrical and Computer Engineering, University of Waterloo, Waterloo, Ont., Canada N2L 3G1

Received 23 January 2003; received in revised form 26 September 2004; accepted 3 April 2005
Available online 16 June 2005

Abstract

In this paper, the presence of transmission delay and sampling delay in chaos-based secure communication systems by employing impulsive synchronization is studied. A time delayed impulsive differential system with delayed impulses, modeling the synchronization error between the driving and response schemes employed in such communication systems, is presented. The equi-attractivity property of the error dynamics is investigated and the sufficient conditions leading to this property are obtained. A set of upper bounds on the delay terms involved in the system are also obtained, and a numerical example is given. A communication security scheme employing hyperchaotic systems possessing continuous driving, impulsive driving and delay is proposed and simulation results are given to demonstrate the performance of the scheme.

Keywords: Impulsive delay systems; Equi-attractivity; Impulsive synchronization; Hyperchaos; Communication security

1. Introduction

Over the past decade, several interesting communication security schemes, based on chaos, have been proposed (Cuomo and Oppenheim, 1993; Grassi and Mascolo, 1999a; Halle et al., 1993; Kocarev et al., 1992; Pecora and Carroll, 1990) for synchronized chaotic and hyperchaotic systems. In these systems, perfect synchronization is usually expected to recover the information signals. In other words, the recovery of the information signals requires the receiver's own copy of the chaotic signal which is synchronized with the transmitter's one. This is done through driving the system at the receiver end by one of the state variables of the system at the transmitter end (Cuomo and Oppenheim, 1993; Halle et al., 1993; Kocarev et al., 1992; Pecora and Carroll, 1990), or by a linear combination of the state variables of the system at the transmitter end (Grassi & Mascolo, 1997, 1999a,b). Therefore, how to achieve synchronization is a key requirement in the design of chaos-based secure communication schemes. In Pecora and Carroll (1990), continuous driving methods and the theory of Lyapunov exponents are applied to study the asymptotic stability of the error system between the driving and response systems. Further investigation of this particular type of synchronization using low-dimensional chaotic systems and employing the Lyapunov-functions theory is given in Cuomo and Oppenheim (1993). The hyperchaos synchronization between higher dimensional chaotic systems, possessing more than one positive Lyapunov exponent, using an observer design method, has been studied in (Grassi & Mascolo, 1997, 1999a,b; Peng et al., 1996). Some theoretical results concerning the conditions under which a specific kind of generalized synchronization whose synchronizing manifold is linear, has been presented in Yang and Chua (1999).

☆ This paper was not presented at any IFAC meeting. This paper was recommended for publication in revised form by Associate Editor E. Leonard under the direction of Editor Hassan Khalil.

* Corresponding author.
E-mail address: anmar.khadra@gmail.com (A. Khadra).

[1] Partially supported by NSERC, Canada.

0005-1098/$ - see front matter © 2005 Elsevier Ltd. All rights reserved.
doi:10.1016/j.automatica.2005.04.012

Another type of synchronization, impulsive synchronization, has been developed (Amritkar and Gupte, 1993; Stojanovski et al., 1996). It allows synchronization of chaotic systems using only small impulses (Suykens et al., 1998; Yang & Chua, 1997a,b) generated by samples of the state variables of the driving system at discrete time instances. These samples are called the synchronizing impulses and they drive the response system discretely at these instances. After a finite period of time, the two chaotic systems behave in accordance with each other and the synchronization of the two chaotic systems is achieved. In other words, the asymptotic stability property of the error dynamics between the driving and response systems is reached. The impulsive synchronization has been applied to a number of chaos-based communication systems which exhibit good performance for the synchronization purposes and for security purposes (Yang & Chua, 1997a,b; Khadra, Liu, & Shen, 2003b). One particular advantage of this approach is its ability to be combined with conventional cryptographic techniques. Recently the detailed experiments and performance analysis of impulsive synchronization have been carried out (Itoh et al., 1999, 2001; Itoh et al., 1999), and synchronization with varying impulse durations has also been studied (Li et al., 2001; Li et al., 2001). However, the transmission and sampling delays in communication security systems employing impulsive synchronization, are inevitable. Therefore it is necessary to analyze the robustness of impulsive synchronization in the presence of these two types of delay. Transmission delay is created from transmitting all the information needed for continuous driving and for accurate decryption of messages. Sampling delay is created from sampling the impulses at the receiver end for identical synchronization. The study of impulsive systems and delayed impulsive systems by employing non-smooth Lyapunov-like functions, has been an active research area for many years. For example, in Ballinger and Liu (1999, 2000), the existence, uniqueness, boundedness and stability of solutions to a specific type of delayed impulsive systems, have been studied by utilizing the theory of Lyapunov functions and Lyapunov functionals. The asymptotic stability of singularly perturbed delayed impulsive systems with uncertainty from non-linear perturbations, is explored in Guan et al. (2001). Actually, delay is an essential issue in communication security systems, especially when dealing with cryptosystems that involve continuous driving as well as impulsive driving. The error dynamics generated from these secure communication systems will involve delay in both the differential system and in the driving impulses simultaneously. In this paper, we investigate the delay issue and the performance of impulsive synchronization under the influence of delay. In particular, we analyze how much delay such systems can endure without losing their desired equi-attractivity properties, and obtain a relationship between the parameters of these systems, including the delay terms. This will reflect the robustness of impulsive synchronization when delay is present and the ability of cryptosystems to overcome the delay problem without affecting their security and performance.

This paper is organized as follows. In Section 2, we present the applications of impulsive synchronization to secure communication and show how delay arises in these models. In Section 3, a general impulsive differential system with delay, which resembles the one used in secure communication and possesses delayed impulses, is presented and the equi-attractivity of its solutions is investigated. In Section 4, a numerical example on impulsive synchronization using a hyperchaotic impulsive system is given to validate the theory obtained in Section 3. A communication security scheme employing hyperchaotic systems is given in Section 5, where additional simulation results are presented to demonstrate the performance of the proposed system. Conclusions are given in Section 6.

2. Problem formulation

A cryptosystem has been proposed in Khadra et al. (2003a), in which the impulses and the encrypted signal are transmitted simultaneously across the public channel. The cryptosystem possesses a response system at the receiver end which is driven continuously by the encrypted signal (transmitted signal), and impulsively by the synchronizing impulses at the discrete instances t_i, $i = 1, 2, \ldots$, where the impulses are applied linearly on the chaotic system at the receiver end. The encryption process is done using chaotic masking and chaotic modulation as follows. If $m(t)$ represents the message signal, then the encrypted signal is given by $f(t) = e(m(t)) = x_1(t)(m(t) + x_3(t))$. The transmitted signal $s(t)$ is a combination of the synchronizing impulses and the encrypted signal $f(t)$. It is used to drive the response system $\mathbf{u}$ continuously and impulsively. Thus due to the presence of transmission delay in the process, a delay term will be involved in the system $\mathbf{u}$ as well as in the impulses, as shown in Fig. 1. Let us denote this type of delay, appearing in the chaotic system $\mathbf{u}$ itself but not in the impulses, by $\widetilde{r}$. Furthermore, sampling the impulses in the chaotic system $\mathbf{u}$ at the receiver end, in order to apply the impulsive synchronization process, will also involve delay. Therefore the impulses at the response system will possess a delay term representing the maximum of the two types

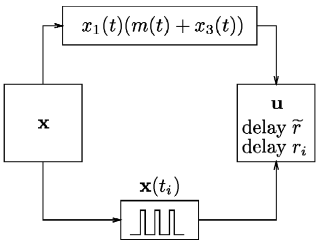

Fig. 1. Cryptosystem involving the transmission of impulses and driving signal $x_1(t)(m(t) + x_3(t))$, with delay.

of delay: transmission delay and sampling delay. We shall denote this maximum delay term by r_i, $i = 1, 2, \ldots$, corresponding to each impulse. If $\mathbf{x}(t_i)$, $i = 1, 2, \ldots$, are the discrete values of the driving system $\mathbf{x}$ sent across a public channel for synchronization, then, using the substitution $\tau_i = t_i + r_i$, for $i = 1, 2, \ldots$, the moments τ_i, $i = 1, 2, \ldots$, become the moments of impulse at the receiver end. Hence the chaotic systems can be represented at the transmitter and the receiver ends, which are based on the Lorenz system and without the presence of the message signal $m(t)$, as follows. At the transmitter end, we have

$$\dot{\mathbf{x}}(t) = A\mathbf{x}(t) + \mathbf{\Phi}_1(\mathbf{x}(t)) + \mathbf{\Phi}_2(\mathbf{x}(t)) \tag{1}$$

and, at the receiver end, we have

$$\begin{cases} \dot{\mathbf{u}}(t) = A\mathbf{u}(t) + \mathbf{\Phi}_1(\mathbf{x}(t-\widetilde{r})) + \mathbf{\Phi}_2(\mathbf{u}(t)), & t \neq \tau_i \\ \Delta\mathbf{u}(t) = -B_i\mathbf{e}(t-r_i), & t = \tau_i, \quad i = 1, 2, \ldots, \end{cases} \tag{2}$$

where

$$A := \begin{pmatrix} -\sigma & \sigma & 0 \\ \rho & -1 & 0 \\ 0 & 0 & -b \end{pmatrix}, \quad \sigma, \rho \text{ and } b \text{ are positive constants,}$$

$\mathbf{\Phi}_1(\mathbf{x}) = (0, -x_1x_3, 0)^{\mathrm{T}}$, $\mathbf{\Phi}_2(\mathbf{x}) = (0, 0, x_1x_2)^{\mathrm{T}}$, $\Delta\mathbf{u}(t_i) = \mathbf{u}(t_i^+) - \mathbf{u}(t_i^-)$, $\mathbf{u}(t_i^+) = \lim_{t\to t_i^+}\mathbf{u}(t)$, B_i are 3×3 constant matrices describing the linear nature of the driving impulses, for $i = 1, 2, \ldots$, and $\mathbf{e} = \mathbf{x} - \mathbf{u}$ is the error dynamics. Notice that according to this model, the system at the receiver end is driven continuously by the signal x_1x_3 and by the impulses. From (1) and (2) the error dynamics $\mathbf{e}$ is given by

$$\begin{cases} \dot{\mathbf{e}}(t) = A\mathbf{e}(t) + \mathbf{\Psi}_1(\mathbf{x}(t), \mathbf{x}(t-\widetilde{r})) \\ \qquad\quad + \mathbf{\Psi}_2(\mathbf{x}(t), \mathbf{u}(t)), \quad t \neq \tau_i, \\ \Delta\mathbf{e}(t) = B_i\mathbf{e}(t-r_i), \quad t = \tau_i, \ i = 1, 2, \ldots, \end{cases} \tag{3}$$

where $\mathbf{\Psi}_1(\mathbf{x}(t), \mathbf{x}(t-\widetilde{r})) = \mathbf{\Phi}_1(\mathbf{x}(t)) - \mathbf{\Phi}_1(\mathbf{x}(t-\widetilde{r}))$ and $\mathbf{\Psi}_2(\mathbf{x}(t), \mathbf{u}(t)) = \mathbf{\Phi}_2(\mathbf{x}(t)) - \mathbf{\Phi}_2(\mathbf{u}(t))$. Let $\sigma = 10$, $\rho = 28$, $b = \frac{8}{3}$, $B_i = B = -\mathrm{diag}(0.5, 0.6, 0.2)$, $\Delta := \Delta_i = \tau_i - \tau_{i-1} = 0.002$, for all $i = 1, 2, \ldots$, and $r_i = \widetilde{r} = 0.001$. By applying the Runge–Kutta integration method with an integration step-size given by 0.0001, identical synchronization cannot be achieved, although the magnitude of the delay is fairly small, as shown in Fig. 2 (a). In fact, choosing different matrices B_i, $i = 1, 2, \ldots$, does not improve the synchronization results. The reason for such behaviour is that the two terms $\mathbf{\Phi}_1(\mathbf{x}(t))$ and $\mathbf{\Phi}_1(\mathbf{x}(t-\widetilde{r}))$ no longer eliminate each other. Thus the magnitude of the error between them will not approach zero, since $\mathbf{x}$ is a chaotic signal. Therefore it is necessary to construct a new system at the receiver end that will synchronize with the chaotic attractor. By adding the two terms $\mathbf{\Phi}_1(\mathbf{u}(t))$ and $-\mathbf{\Phi}_1(\mathbf{u}(t-\widetilde{r}))$ in (2), we obtain

$$\begin{cases} \dot{\mathbf{u}}(t) = A\mathbf{u}(t) + \mathbf{\Phi}_1(\mathbf{u}(t)) + \mathbf{\Phi}_1(\mathbf{x}(t-\widetilde{r})) \\ \qquad\quad - \mathbf{\Phi}_1(\mathbf{u}(t-\widetilde{r})) + \mathbf{\Phi}_2(\mathbf{u}(t)), \quad t \neq \tau_i, \\ \Delta\mathbf{u}(t) = -B_i\mathbf{e}(t-r_i), \quad t = \tau_i, \ i = 1, 2, \ldots. \end{cases} \tag{4}$$

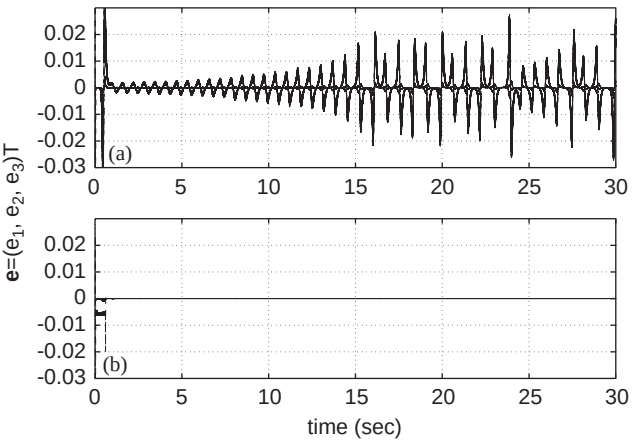

Fig. 2. Error dynamics (a) for system (3); (b) for system (4).

This is feasible because the two terms are generated using the response system at the receiver end and are also independent of the system at the transmitter end. Upon the addition of these two terms, the error dynamics is given by

$$\begin{cases} \dot{\mathbf{e}}(t) = A\mathbf{e}(t) + \mathbf{\Psi}_1(\mathbf{x}(t), \mathbf{u}(t)) + \mathbf{\Psi}_1(\mathbf{x}(t-\widetilde{r}), \\ \qquad\quad \mathbf{u}(t-\widetilde{r})) + \mathbf{\Psi}_2(\mathbf{x}(t), \mathbf{u}(t)), \quad t \neq \tau_i, \\ \Delta\mathbf{e}(t) = B_i\mathbf{e}(t-r_i), \quad t = \tau_i, \ i = 1, 2, \ldots. \end{cases} \tag{5}$$

The simulation of the error dynamics, given by (5), using the same values given above except for the delay terms, where we have chosen $r_i = 0.002$, $i = 1, 2, \ldots$, and $\widetilde{r} = 0.6$, shows identical synchronization (see Fig. 2(b)).

We shall analyze the dynamics of system (5) and find the conditions under which the equi-attractivity property of this system may be achieved. First, we state the following observations:

1. Notice that

   $$\|\mathbf{\Psi}_m(\mathbf{x}, \mathbf{u})\| \leqslant L_m\|\mathbf{x} - \mathbf{u}\| = L_m\|\mathbf{e}\|,$$

   where $m = 1, 2$ and L_1 and L_2 are two positive constants. The later inequality will be used in the theory developed for a certain kind of ODEs.
2. Due to the presence of delay in system (5), we shall employ two different types of norms where appropriate, the standard Euclidean norm $\|\mathbf{x}(t)\|$ and the supremum norm defined by

   $$\|\mathbf{x}_t\|_{\widetilde{r}} = \sup_{s\in[-\widetilde{r},0]} \|\mathbf{x}(t+s)\|,$$

   where $\mathbf{x}_t(s) = \mathbf{x}(t+s)$, for all $s \in [-\widetilde{r}, 0]$. The later norm and the notation $\mathbf{x}_t$ are standard mathematical tools used in the theory of delayed differential equations. Note that $\|\mathbf{x}(t)\| \leqslant \|\mathbf{x}_t\|_{\widetilde{r}}$, and it will be used in the later development of the theory.

3. Stability of delayed impulsive systems

Consider the system

$$\left\{\begin{array}{l}\dot{\mathbf{x}}(t)=A\mathbf{x}(t)+\boldsymbol{\Psi}_1(\mathbf{x}(t))+\boldsymbol{\Psi}_1(\mathbf{x}(t-\widetilde{r}))\\ \qquad\quad +\boldsymbol{\Psi}_2(\mathbf{x}(t)), \quad t\neq\tau_i,\\ \Delta\mathbf{x}(t)=B_i\mathbf{x}(t-r_i), \quad t=\tau_i\ i=1,2,\ldots,\\ \mathbf{x}(t)=\boldsymbol{\phi}(t-t_0),\ t_0-r\leqslant t\leqslant t_0,\end{array}\right\}\quad t>t_0, \tag{6}$$

where A is an $n\times n$ constant matrix, $\Delta\mathbf{x}(\tau_i)=\mathbf{x}(\tau_i^+)-\mathbf{x}(\tau_i^-)$, $\mathbf{x}(\tau_i^+)=\lim_{t\to\tau_i^+}\mathbf{x}(t)$, the moments of impulse satisfy $t_0<\tau_1<\tau_2<\cdots<\tau_i<\ldots$ and $\lim_{i\to\infty}\tau_i=\infty$, $\boldsymbol{\phi}(t)$ is a continuous initial function defined over $[t_0-r,t_0]$, $\widetilde{r}$ and r_i are constant delay terms, for all $i=1,2,\ldots,$ and $r:=\max_i\{\widetilde{r},r_i\}\geqslant 0$. Let $k,\widetilde{k},k_i,\ i=1,2,\ldots,$ be a set of non-negative integers chosen in such a way that $\tau_{i-k}<\tau_i-r\leqslant\tau_{i-k+1}$, $\tau_{i-k_i}<\tau_i-r_i\leqslant\tau_{i-k_i+1}$ and $\tau_{i-\widetilde{k}}<\tau_i-\widetilde{r}\leqslant\tau_{i-\widetilde{k}+1}$, where $1\leqslant k_i+\widetilde{k}\leqslant i$ and τ_0 is defined to be some point satisfying $t_0-r\leqslant\tau_0<\tau_1$ (notice that τ_0 does not represent a moment of impulse). Assume that $\boldsymbol{\Psi}_1$ and $\boldsymbol{\Psi}_2$ are continuous non-linear maps satisfying $\|\boldsymbol{\Psi}_m(\mathbf{x})\|\leqslant L_m\|\mathbf{x}\|$, where $m=1$ or 2, for some L_1 and $L_2>0$, and B_i are $n\times n$ constant matrices satisfying $\|B_i\|=\sqrt{\lambda_{\max}(B_i^{\mathrm{T}}B_i)}<L_3$, for all $i=1,2,\ldots,$ and for some $L_3>0$ ($\lambda_{\max}(B^{\mathrm{T}}B)$ is the largest eigenvalue of $B^{\mathrm{T}}B$). This guarantees that, for each $(t_0,\boldsymbol{\phi})\in\mathbb{R}_+\times C([-r,0],\mathbb{R}^n)$, there exists a local solution of (6) satisfying the initial condition $\mathbf{x}(t)=\boldsymbol{\phi}(t-t_0)$, for $t_0-r\leqslant t\leqslant t_0$ (Ballinger and Liu, 1999, 2000). Let $\mathbf{x}(t):=\mathbf{x}(t,t_0,\boldsymbol{\phi})$ be any solution of (6) satisfying $\mathbf{x}(t)=\boldsymbol{\phi}(t-t_0)$, for $t_0-r\leqslant t\leqslant t_0$, and $\mathbf{x}(t)$ be left continuous at each $\tau_i>t_0$ in the interval of existence, i.e., $\mathbf{x}(\tau_i^-)=\mathbf{x}(\tau_i)$. In order to state the main result, we shall introduce the following classes of functions and some necessary definitions:

$$S^{\mathrm{c}}(M):=\{\mathbf{x}\in\mathbb{R}^n:\|\mathbf{x}\|\geqslant M\},$$

$$S^{\mathrm{c}}(M)^0:=\{\mathbf{x}\in\mathbb{R}^n:\|\mathbf{x}\|>M\},$$

$$v_0(M):=\{V:\mathbb{R}_+\times S^{\mathrm{c}}(M)\to\mathbb{R}_+:V(t,\mathbf{x})\in C((t_k,t_{k+1}]\times S^{\mathrm{c}}(M)),\text{ locally Lipschitz in }\mathbf{x}\text{ and }V(t_k^+,\mathbf{x})\text{ exists for }k=1,2,\ldots\},\text{ where }M\geqslant 0.$$

Definition 1. Given the delay constant r, the linear space $C([-r,0],\mathbb{R}^n)$ is equipped with the norm $\|\cdot\|_r$ defined by $\|\boldsymbol{\phi}\|_r=\sup_{-r\leqslant s\leqslant 0}\|\boldsymbol{\phi}(s)\|$.

Definition 2. Let $M\geqslant 0$ and $V\in v_0(M)$. Define the upper right derivative of $V(t,\mathbf{x})$ with respect to the continuous portion of system (6), for $(t,\mathbf{x})\in\mathbb{R}_+\times S^{\mathrm{c}}(M)^0$ and $t\neq\tau_i$, by

$$D^+V(t,\mathbf{x}):=\lim_{\delta\to 0^+}\sup\frac{1}{\delta}[V(t+\delta,\mathbf{x}+\delta\mathbf{f}(t,\mathbf{x}))-V(t,\mathbf{x})].$$

Definition 3. Solutions of the impulsive system (6) are said to be

(S1) equi-attractive in the large if for each $\varepsilon>0$, $\alpha>0$ and $t_0\in\mathbb{R}_+$, there exists a number $T:=T(t_0,\varepsilon,\alpha)>0$ such that $\|\boldsymbol{\phi}\|_r<\alpha$ implies $\|\mathbf{x}(t)\|<\varepsilon$, for $t\geqslant t_0+T$;
(S2) uniformly equi-attractive in the large if T in (S1) is independent of t_0.

From the definition of equi-attractivity in the large, it can be seen that solutions of system (6), which possess this property, will converge to zero no matter how large $\|\boldsymbol{\phi}\|_r$ is, i.e., $\lim_{t\to\infty}\mathbf{x}(t)=\mathbf{0}$. Moreover, the notions of uniform equi-attractivity in the large and equi-attractivity in the large become identical for autonomous systems. Therefore the term uniform is dropped. Furthermore, equi-attractivity in the large will be an appropriate tool for reflecting the behaviour of impulsive synchronization of chaotic systems (1) and (4), by driving the error dynamics (5) to zero.

Notice that by applying Taylor's Theorem, Taylor's Remainder Theorem and system (6), we obtain the estimate

$$\begin{aligned}\mathbf{x}(\tau_i-r_i)&=\mathbf{x}(\tau_i)-r_i\dot{\mathbf{x}}(t)\\ &=\mathbf{x}(\tau_i)-r_iA\mathbf{x}(t)-r_i\boldsymbol{\Psi}_1(\mathbf{x}(t))\\ &\quad -r_i\boldsymbol{\Psi}_1(\mathbf{x}(t-\widetilde{r}))-r_i\boldsymbol{\Psi}_2(\mathbf{x}(t))\end{aligned}$$

for small r_i and for some $t\in(\tau_i-r_i,\tau_i)$, $i=1,2,\ldots$. If t is one of the impulses, then $\dot{\mathbf{x}}(t)$ refers to the left hand derivative which exists. It follows that

$$\begin{aligned}\|\mathbf{x}(\tau_i)-\mathbf{x}(\tau_i-r_i)\|&\leqslant r_i[\|A\|+L_1+L_2]\|\mathbf{x}(t)\|\\ &\quad +r_iL_1\|\mathbf{x}(t-\widetilde{r})\|\end{aligned}\tag{7}$$

for some $t\in(\tau_i-r_i,\tau_i)$ and for $i=1,2,\ldots$. The importance of inequality (7) will become evident in the proof of the next theorem which will give the conditions under which system (6) is equi-attractive in the large.

Theorem 4. *Let $2\widetilde{\lambda}$ be the largest eigenvalue of $A^{\mathrm{T}}+A$, $\Delta_{i+1}:=\tau_{i+1}-\tau_i\leqslant\Delta$, for some $\Delta>0$,*

$$\mathscr{E}_i:=\mathscr{K}_i\|I+B_i\|,\tag{8}$$

$$\mathscr{F}_i:=r_i\mathscr{L}_i\|B_i\|[\|A\|+2L_1+L_2],\tag{9}$$

$$\mathscr{K}_i:=\exp\{a\Delta_{i+1}+L_1\Delta_{i+1}\exp(a\Delta_{i+1})\},\tag{10}$$

$$\mathscr{L}_i:=\exp\left\{a(\tau_i-\tau_{i-k_i-\widetilde{k}})+\frac{L_1}{a}\times\exp[a(\tau_i-\tau_{i-k_i-\widetilde{k}})]-\frac{L_1}{a}\right\}\tag{11}$$

for $i=1,2,\ldots,$ where $a:=\widetilde{\lambda}+L_1+L_2$ and I is the identity matrix of an appropriate dimension. If J_i is the

$(k_i+\widetilde{k})\times(k_i+\widetilde{k})$ *matrix given by*

$$J_i:=\begin{pmatrix} 0 & 1 & 0 & \cdots & 0 & \cdots & 0 & 0\\ 0 & 0 & 1 & \cdots & 0 & \cdots & 0 & 0\\ 0 & 0 & 0 & \cdots & 0 & \cdots & 0 & 0\\ \vdots & \vdots & \vdots & \ddots & \vdots & \ddots & \vdots & \vdots\\ 0 & 0 & 0 & \cdots & 0 & \cdots & 0 & 1\\ \mathscr{F}_i & 0 & 0 & \cdots & \mathscr{E}_i & \cdots & 0 & 0 \end{pmatrix}, \tag{12}$$

$i=1,2,\ldots,$ *where* $\mathscr{E}_i$ *is in the* k_ith *column, then system* (6) *is equi-attractive in the large provided that every eigenvalue,* $\lambda^{(i)}$*, of* J_i *satisfies* $|\lambda^{(i)}|\leqslant\gamma<1$*, for* $i=1,2,\ldots$ *(in other words, the matrix* J_i *may define a contraction linear mapping over* $\mathbb{R}^{k_i+\widetilde{k}}$*).*

Proof. We shall prove that under the assumptions of Theorem 4, $\|\mathbf{x}_t\|_{\widetilde{r}}\to 0$, as $t\to\infty$. Thus, in view of observation 2 in the previous section, we can immediately conclude that $\|\mathbf{x}(t)\|\to 0$, as $t\to\infty$ which means that system (6) is equi-attractive in the large. By considering the Euclidean norm $V(\mathbf{x}(t)):=\|\mathbf{x}(t)\|=(\mathbf{x}^{\mathrm{T}}\mathbf{x})^{1/2}$, we have

$$\begin{aligned} D^+V(\mathbf{x}) &= (1/2)(\mathbf{x}^{\mathrm{T}}\mathbf{x})^{-1/2}(\dot{\mathbf{x}}^{\mathrm{T}}\mathbf{x}+\mathbf{x}^{\mathrm{T}}\dot{\mathbf{x}})\\ &= (1/2\|\mathbf{x}\|)[\mathbf{x}^{\mathrm{T}}(A^{\mathrm{T}}+A)\mathbf{x}+2\boldsymbol{\Psi}_1(\mathbf{x})^{\mathrm{T}}\mathbf{x}\\ &\quad +2\boldsymbol{\Psi}_1(\mathbf{x}(t-\widetilde{r}))^{\mathrm{T}}\mathbf{x}+2\boldsymbol{\Psi}_2(\mathbf{x})^{\mathrm{T}}\mathbf{x}]\\ &\leqslant (1/2\|\mathbf{x}\|)[2\widetilde{\lambda}\|\mathbf{x}\|^2+2L_1\|\mathbf{x}\|^2+2L_2\|\mathbf{x}\|^2\\ &\quad +2\|\boldsymbol{\Psi}_1(\mathbf{x}(t-\widetilde{r}))\|\|\mathbf{x}\|]\\ &\leqslant (\widetilde{\lambda}+L_1+L_2)\|\mathbf{x}\|+L_1\|\mathbf{x}(t-\widetilde{r})\|. \end{aligned}$$

i.e., $D^+[\|\mathbf{x}(t)\|]\leqslant a\|\mathbf{x}(t)\|+L_1\|\mathbf{x}(t-\widetilde{r})\|$, which implies that

$$D^+[\|\mathbf{x}(t)\|]-a\|\mathbf{x}(t)\|\leqslant L_1\|\mathbf{x}(t-\widetilde{r})\|.$$

Multiplying both sides of the above inequality by $\exp(-at)$, we obtain

$$\mathrm{e}^{-at}D^+[\|\mathbf{x}(t)\|]-a\mathrm{e}^{-at}\|\mathbf{x}(t)\|\leqslant L_1\mathrm{e}^{-at}\|\mathbf{x}(t-\widetilde{r})\|.$$

This implies that

$$D^+[\mathrm{e}^{-at}\|\mathbf{x}(t)\|]\leqslant L_1\mathrm{e}^{-at}\|\mathbf{x}(t-\widetilde{r})\|. \tag{13}$$

Therefore, for every $t\in(\tau_i-r_i,\tau_i]\subset(\tau_{i-k_i},\tau_i]$, for every $s\in[-\widetilde{r},0]$ and for every $i=1,2,\ldots,$ we have $t+s\in(\tau_{i-k_i}-\widetilde{r},\tau_i]\subset(\tau_{i-k_i-\widetilde{k}},\tau_i]$, where $t-\widetilde{r}>\tau_{i-k_i-\widetilde{k}}$, and, by (13),

$$\begin{aligned} &\int_{\tau^+_{i-k_i-\widetilde{k}}}^{t+s} D^+[\mathrm{e}^{-a\tau}\|\mathbf{x}(\tau)\|]\,\mathrm{d}\tau\\ &\quad\leqslant L_1\int_{\tau^+_{i-k_i-\widetilde{k}}}^{t+s}\mathrm{e}^{-a\tau}\|\mathbf{x}(\tau-\widetilde{r})\|\,\mathrm{d}\tau. \end{aligned}$$

Hence

$$\begin{aligned} \|\mathbf{x}_t(s)\| &\leqslant \mathrm{e}^{a(t+s-\tau_{i-k_i-\widetilde{k}})}\|\mathbf{x}(\tau^+_{i-k_i-\widetilde{k}})\|\\ &\quad +L_1\int_{\tau^+_{i-k_i-\widetilde{k}}}^{t+s}\mathrm{e}^{a(t+s-\tau)}\|\mathbf{x}_\tau\|_{\widetilde{r}}\,\mathrm{d}\tau. \end{aligned}$$

Taking the supremum of both sides of the latter inequality over $s\in[-\widetilde{r},0]$, we obtain

$$\begin{aligned} &\sup_{s\in[-\widetilde{r},0]}\|\mathbf{x}_t(s)\|\\ &\leqslant \sup_{s\in[-\widetilde{r},0]}\left\{\mathrm{e}^{a(t+s-\tau_{i-k_i-\widetilde{k}})}\|\mathbf{x}(\tau^+_{i-k_i-\widetilde{k}})\|\right.\\ &\quad \left.+L_1\int_{\tau^+_{i-k_i-\widetilde{k}}}^{t+s}\mathrm{e}^{a(t+s-\tau)}\|\mathbf{x}_\tau\|_{\widetilde{r}}\,\mathrm{d}\tau\right\}\\ &\leqslant \mathrm{e}^{a(\tau_i-\tau_{i-k_i-\widetilde{k}})}\|\mathbf{x}(\tau^+_{i-k_i-\widetilde{k}})\|\\ &\quad +L_1\int_{\tau^+_{i-k_i-\widetilde{k}}}^{t}\mathrm{e}^{a(t-\tau)}\|\mathbf{x}_\tau\|_{\widetilde{r}}\,\mathrm{d}\tau. \end{aligned}$$

Thus

$$\begin{aligned} \|\mathbf{x}_t\|_{\widetilde{r}} &\leqslant \mathrm{e}^{a(\tau_i-\tau_{i-k_i-\widetilde{k}})}\|\mathbf{x}(\tau^+_{i-k_i-\widetilde{k}})\|\\ &\quad +L_1\int_{\tau^+_{i-k_i-\widetilde{k}}}^{t}\mathrm{e}^{a(t-\tau)}\|\mathbf{x}_\tau\|_{\widetilde{r}}\,\mathrm{d}\tau. \end{aligned}$$

Applying Gronwall's Lemma (Lakshmikantham and Liu, 1993) and Eq. (11), we obtain

$$\begin{aligned} \|\mathbf{x}_t\|_{\widetilde{r}} &\leqslant \mathrm{e}^{a(\tau_i-\tau_{i-k_i-\widetilde{k}})}\|\mathbf{x}(\tau^+_{i-k_i-\widetilde{k}})\|\exp\\ &\quad\times\left[L_1\int_{\tau_{i-k_i-\widetilde{k}}}^{t}\mathrm{e}^{a(t-\tau)}\,\mathrm{d}\tau\right]\\ &\leqslant \mathscr{L}_i\|\mathbf{x}(\tau^+_{i-k_i-\widetilde{k}})\|. \end{aligned}$$

By observation 2, it follows, for every $t\in(\tau_i-r_i,\tau_i]\subset(\tau_{i-k_i},\tau_i]$ and $i=1,2,\ldots,$ that

$$\|\mathbf{x}(t)\|\leqslant\|\mathbf{x}_t\|_{\widetilde{r}}\leqslant\mathscr{L}_i\|\mathbf{x}(\tau^+_{i-k_i-\widetilde{k}})\|. \tag{14}$$

Similarly, by inequality (13) and for all $t\in(\tau_i,\tau_{i+1}]$, $s\in[-\widetilde{r},0]$ and $i=1,2,\ldots,$ where $t+s\in(\tau_i-\widetilde{r},\tau_i]\subset(\tau_{i-\widetilde{k}},\tau_i]$, we have

$$\begin{aligned} &\int_{\tau^+_{i-\widetilde{k}}}^{t+s} D^+[\mathrm{e}^{-a\tau}\|\mathbf{x}(\tau)\|]\,\mathrm{d}\tau\\ &\quad\leqslant L_1\int_{\tau^+_{i-\widetilde{k}}}^{t+s}\mathrm{e}^{-a\tau}\|\mathbf{x}(\tau-\widetilde{r})\|\,\mathrm{d}\tau. \end{aligned}$$

It follows that

$$\begin{aligned} &\sup_{s\in[-\widetilde{r},0]}\|\mathbf{x}_t(s)\|\\ &\leqslant \sup_{s\in[-\widetilde{r},0]}\left\{\mathrm{e}^{a(t+s-\tau_i)}\|\mathbf{x}(\tau^+_{i-\widetilde{k}})\|\right.\\ &\quad \left.+L_1\int_{\tau^+_{i-\widetilde{k}}}^{t+s}\mathrm{e}^{a(t+s-\tau)}\|\mathbf{x}_\tau\|_{\widetilde{r}}\,\mathrm{d}\tau\right\}. \end{aligned}$$

Thus

$$\|\mathbf{x}_t\|_{\widetilde{r}} \leqslant \mathrm{e}^{a(t-\tau_i)}\|\mathbf{x}(\tau_{i-\widetilde{k}}^+)\| + L_1\int_{\tau_{i-\widetilde{k}}^+}^{t} \mathrm{e}^{a(t-\tau)}\|\mathbf{x}_\tau\|_{\widetilde{r}}\,\mathrm{d}\tau$$
$$\leqslant \mathrm{e}^{a\Delta_{i+1}}\|\mathbf{x}(\tau_{i-\widetilde{k}}^+)\| + L_1\mathrm{e}^{a\Delta_{i+1}}\int_{\tau_{i-\widetilde{k}}^+}^{t} \|\mathbf{x}_\tau\|_{\widetilde{r}}\,\mathrm{d}\tau.$$

It follows, by Gronwall's Lemma and Eq. (10), for all $i=1, 2, \ldots$, that

$$\|\mathbf{x}_t\|_{\widetilde{r}} \leqslant \exp[a\Delta_{i+1} + L_1\Delta_{i+1}\mathrm{e}^{a\Delta_{i+1}}]\|\mathbf{x}(\tau_{i-\widetilde{k}}^+)\| = \mathscr{K}_i\|\mathbf{x}(\tau_{i-\widetilde{k}}^+)\|.$$

Passing to the limit as $t \to \tau_{i+1}$, $i=1, 2, \ldots$, the later inequality becomes

$$\|\mathbf{x}_{\tau_{i+1}}\|_{\widetilde{r}} \leqslant \mathscr{K}_i\|\mathbf{x}(\tau_{i-\widetilde{k}}^+)\|. \tag{15}$$

On the other hand, by system (6), Eq. (7) and observation 2, we have, for $i=1, 2, \ldots$,

$$\begin{aligned}\|\mathbf{x}(\tau_i^+)\| &= \|\mathbf{x}(\tau_i) + B_i\mathbf{x}(\tau_i - r_i)\|\\ &\leqslant \|I + B_i\|\|\mathbf{x}(\tau_i)\| + \|B_i\|\|\mathbf{x}(\tau_i) - \mathbf{x}(\tau_i - r_i)\|\\ &\leqslant \|I + B_i\|\|\mathbf{x}(\tau_i)\| + r_i\|B_i\|(\|A\|\\ &\quad + L_1 + L_2)\|\mathbf{x}(t)\| + r_iL_1\|B_i\|\|\mathbf{x}(t-\widetilde{r})\|\\ &\leqslant \|I + B_i\|\|\mathbf{x}(\tau_i)\| + r_i\|B_i\|(\|A\|\\ &\quad + L_1 + L_2)\|\mathbf{x}(t)\| + r_iL_1\|B_i\|\|\mathbf{x}_t\|_{\widetilde{r}}.\end{aligned}$$

By applying inequality (14), we get

$$\|\mathbf{x}(\tau_i^+)\| \leqslant \|I + B_i\|\|\mathbf{x}(\tau_i)\| + r_i\mathscr{L}_i\|B_i\|(\|A\| + 2L_1 + L_2)\|\mathbf{x}(\tau_{i-k_i-\widetilde{k}}^+)\|.$$

Hence, by Eqs. (8), (9) and inequality (15), together with observation 2, we have, for $i=1, 2, \ldots$,

$$\begin{aligned}\|\mathbf{x}(\tau_i^+)\| &\leqslant \mathscr{K}_i\|I + B_i\|\|\mathbf{x}(\tau_{i-\widetilde{k}-1}^+)\|\\ &\quad + r_i\mathscr{L}_i\|B_i\|(\|A\| + 2L_1 + L_2)\|\mathbf{x}(\tau_{i-k_i-\widetilde{k}}^+)\|\\ &= \mathscr{E}_i\|\mathbf{x}(\tau_{i-\widetilde{k}-1}^+)\| + \mathscr{F}_i\|\mathbf{x}(\tau_{i-k_i-\widetilde{k}}^+)\|.\end{aligned} \tag{16}$$

Let $v_1(i-k_i) := \|\mathbf{x}(\tau_{i-k_i-\widetilde{k}}^+)\|$, $v_2(i-k_i) := \|\mathbf{x}(\tau_{i-k_i-\widetilde{k}+1}^+)\|, \ldots, v_{k_i+\widetilde{k}+1}(i-k_i) := \|\mathbf{x}(\tau_i^+)\|$, for all $i=1, 2, \ldots$. By inequality (16), it follows that $v_1(i-k_i+1) = v_2(i-k_i)$, $v_2(i-k_i+1) = v_3(i-k_i), \ldots, v_{k_i+\widetilde{k}-1}(i-k_i+1) = v_{k_i+\widetilde{k}}(i-k_i)$ and $v_{k_i+\widetilde{k}}(i-k_i+1) \leqslant \mathscr{E}_i v_{k_i}(i-k_i) + \mathscr{F}_i v_1(i-k_i)$, $i=1, 2, \ldots$. Define the vector $\mathbf{v}(i) := (v_1(i), v_2(i), \ldots, v_{k_i+\widetilde{k}}(i))^{\mathrm{T}} \in \mathbb{R}^{k_i+\widetilde{k}}$, $i=1, 2, \ldots$. Then the system of difference inequalities obtained above may be written in a matrix form as follows:

$$\mathbf{v}(i-k_i+1) \leqslant J_i\mathbf{v}(i-k_i), \tag{17}$$

$i=1, 2, \ldots$, where J_i is defined by Eq. (12). Thus if each eigenvalue, $\lambda^{(i)}$, of J_i lies strictly inside the unit circle, i.e., $|\lambda^{(i)}| \leqslant \gamma < 1$, $i=1, 2, \ldots$, then the matrix J_i may define a contraction mapping. Since each $k_i \leqslant k$, for all $i=1, 2, \ldots$, it follows, by (17), that $\lim_{i\to\infty}\mathbf{v}(i) = \mathbf{0}$. On the other hand, $v_{k_i+\widetilde{k}+1}(i-k_i) = \|\mathbf{x}(\tau_i^+)\|$, $i=1, 2, \ldots$. Therefore we can conclude that

$$\lim_{i\to\infty}\|\mathbf{x}(\tau_i^+)\| = \lim_{i\to\infty} v_{k_i+\widetilde{k}+1}(i-k_i) = \lim_{i\to\infty} v_{\widetilde{k}+1}(i) = 0.$$

Moreover, from inequality (14), we can further conclude that, for every $t \in (\tau_i - r_i, \tau_i]$, $i=1, 2, \ldots$,

$$\|\mathbf{x}(t)\| \leqslant \|\mathbf{x}_t\|_{\widetilde{r}} \leqslant \mathscr{L}_i\|\mathbf{x}(\tau_{i-k_i-\widetilde{k}}^+)\| \to 0,$$

as $i \to \infty$, where it is clear that $\mathscr{L}_i$ has an upper bound, for all $i=1, 2, \ldots$. In other words $\|\mathbf{x}(t)\| \to 0$, as $t \to \infty$. Thus solutions to system (6) are equi-attractive in the large, as required. □

With the absence of the delay term $\widetilde{r}$ from (6), the resulting system is an impulsive system with delayed impulses, given by

$$\left\{\begin{array}{ll}\dot{\mathbf{x}}(t) = A\mathbf{x}(t) + \mathbf{\Phi}(\mathbf{x}(t)), & t \neq \tau_i,\\ \Delta\mathbf{x}(t) = B_i\mathbf{x}(t-r_i), & t = \tau_i,\\ \mathbf{x}(t) = \boldsymbol{\phi}(t-t_0), & \end{array}\right\} \begin{array}{l} t > t_0,\\ \\ t_0 - r \leqslant t \leqslant t_0.\end{array} \tag{18}$$

Theorem 4 can be applied to system (18) in the following manner. By comparing system (6) with (18), we obtain $\widetilde{r}=0$, $\widetilde{k}=0$, $\mathbf{\Psi}_1(\mathbf{x}) = \mathbf{0}$ and $\mathbf{\Psi}_2(\mathbf{x}) = \mathbf{\Phi}(\mathbf{x})$. This implies that $\|\mathbf{\Phi}(\mathbf{x})\| \leqslant L_2\|\mathbf{x}\|$ and $L_1 = 0$. In this case, according to Theorem 4, the result that corresponds to system (18) is described by the following corollary.

Corollary 5. *Let $2\widetilde{\lambda}$ be the largest eigenvalue of $A^{\mathrm{T}} + A$, $\Delta_{i+1} \leqslant \Delta$, for some $\Delta > 0$,*

$$\mathscr{E}_i = \mathrm{e}^{d\Delta_{i+1}}\|I + B_i\|,$$

$$\mathscr{F}_i = r_i\mathrm{e}^{d(\Delta_{i+1}+\tau_i-\tau_{i-k_i})}\|B_i\|[\|A\| + L_2]$$

for $i=1, 2, \ldots$, where $d := \widetilde{\lambda} + L_2$. If J_i is the $k_i \times k_i$ matrix given by

$$J_i := \begin{pmatrix} 0 & 1 & 0 & \cdots & 0 & 0\\ 0 & 0 & 1 & \cdots & 0 & 0\\ 0 & 0 & 0 & \cdots & 0 & 0\\ \vdots & \vdots & \vdots & \ddots & \vdots & \vdots\\ 0 & 0 & 0 & \cdots & 0 & 1\\ \mathscr{F}_i & 0 & 0 & \cdots & 0 & \mathscr{E}_i \end{pmatrix},$$

$i=1, 2, \ldots$, then system (18) *is equi-attractive in the large provided that each eigenvalue, $\lambda^{(i)}$, of J_i satisfies $|\lambda^{(i)}| \leqslant \gamma < 1$, $i=1, 2, \ldots$.*

Proof. The proof follows directly from Theorem 4 and the fact that $\widetilde{r}=0$, $\widetilde{k}=0$ and $\mathbf{\Psi}_1(\mathbf{x}) = \mathbf{0}$. □

We shall now state four useful remarks regarding the results of Theorem 4 and Corollary 5.

Remark 1. The eigenvalues of the matrix J_i, for all $i = 1, 2, \ldots$, are the roots of the characteristic equation, given by

$$(\lambda^{(i)})^{k_i}[(\lambda^{(i)})^{\widetilde{k}} - \mathscr{E}_i] - \mathscr{F}_i = 0.$$

Therefore, as the delay term $\widetilde{r}$ increases, the dimension of the matrix J_i also increases and thus the degree of the characteristic polynomial will increase.

Remark 2. Theorem 4 and Corollary 5 can be used to choose appropriate matrices B_i, $i = 1, 2, \ldots$, which make the eigenvalues, $\lambda^{(i)}$, of J_i lie inside the unit circle. Furthermore, if the matrices B_i, $i = 1, 2, \ldots$, are given, then Theorem 4 and Corollary 5 can also provide an upper bound on the delay terms r_i, $i = 1, 2, \ldots$, for which systems (6) and (18) remain equi-attractive in the large.

Remark 3. Although, intuitively, one may conclude that the delay term $\widetilde{r}$ has no influence on the dynamics of the impulsive system, Theorem 4 indicates that the value of $\mathscr{L}_i$ and the dimension of the matrix J_i, for $i = 1, 2, \ldots$, will increase as the value $\widetilde{r}$ increases. Thus the upper bound on the range of values of r_i will change accordingly so that system (6) will remain equi-attractive in the large. We will show, through several numerical examples in the next section, that when considering impulsive synchronization of hyperchaotic systems, the larger the delay term $\widetilde{r}$, the smaller the upper bound on the delay terms r_i, $i = 1, 2, \ldots$, in order to obtain identical synchronization.

Remark 4. The conditions of Theorem 1 and Corollary 1 are all sufficient conditions but not necessary, i.e., systems (6) and (18) may remain equi-attractive in the large, although one of the conditions of Theorem 4 and Corollary 5 may fail. This is also illustrated through numerical examples in the next section when considering impulsive synchronization.

4. Examples on hyperchaos synchronization

Recently, hyperchaotic systems have gained considerable attention for their potential applications to the field of secure communication. Due to the fact that hyperchaotic systems possess more than one positive Lyapunov exponent (unlike low-dimensional chaotic systems), it is believed that hyperchaos might be a better tool for constructing a chaos-based secure communication scheme. In this section, we shall present several examples to investigate impulsive synchronization of two four-dimensional hyperchaotic systems with the presence of delay, in order to apply the theory obtained in the previous section.

Hyperchaos was observed for the first time in 1986 from a real physical system—a fourth order electrical circuit (Matsumoto et al., 1986). This simple circuit is autonomous and contains only one non-linear element, a three-segment piecewise-linear resistor. All other elements are linear and passive, except an active resistor, which has a negative resistance. By considering the circuit parameters from (Matsumoto et al., 1986), the dynamics can be written as

$$\begin{pmatrix}\dot{x}_1\\ \dot{x}_2\\ \dot{x}_3\\ \dot{x}_4\end{pmatrix} = \begin{pmatrix}0 & 0 & -2 & 0\\ 0 & 0 & 0 & -20\\ 1 & 0 & 1 & 0\\ 0 & 1.5 & 0 & 0\end{pmatrix}\begin{pmatrix}x_1\\ x_2\\ x_3\\ x_4\end{pmatrix} + \begin{pmatrix}2g(x_2 - x_1)\\ -20g(x_2 - x_1)\\ 0\\ 0\end{pmatrix}, \tag{19}$$

where x_1 and x_2 denote the voltage across the two capacitors in the circuit, whereas x_3 and x_4 denote the currents through the two inductors included in the same circuit. The mapping g is a piecewise-linear function, given by

$$g(x_2 - x_1) = 3(x_2 - x_1) - 1.6(|x_2 - x_1 + 1| - |x_2 - x_1 - 1|). \tag{20}$$

Let $\mathbf{\Phi}_1(\mathbf{x}) = [0, -20g(x_2 - x_1), 0, 0]^{\mathrm{T}}$, $\mathbf{\Phi}_2(\mathbf{x}) = [2g(x_2 - x_1), 0, 0, 0]^{\mathrm{T}}$ and

$$A = \begin{pmatrix}0 & 0 & -2 & 0\\ 0 & 0 & 0 & -20\\ 1 & 0 & 1 & 0\\ 0 & 1.5 & 0 & 0\end{pmatrix}.$$

Then system (19) becomes

$$\dot{\mathbf{x}}(t) = A\mathbf{x}(t) + \mathbf{\Phi}_1(\mathbf{x}(t)) + \mathbf{\Phi}_2(\mathbf{x}(t)). \tag{21}$$

System (21) will represent the driving system in our model, whereas the response system will be given by

$$\begin{cases}\dot{\mathbf{u}}(t) = A\mathbf{u}(t) + \mathbf{\Phi}_1(\mathbf{u}(t)) + \mathbf{\Phi}_1(\mathbf{x}(t-\widetilde{r})) - \mathbf{\Phi}_1(\mathbf{u}(t-\widetilde{r})) + \mathbf{\Phi}_2(\mathbf{u}(t)), & t \neq \tau_i,\\ \Delta\mathbf{u}(t) = -B_i\mathbf{e}(t - r_i), & t = \tau_i,\ i = 1, 2, \ldots,\end{cases} \tag{22}$$

where $\mathbf{e}(t) = \mathbf{x}(t) - \mathbf{u}(t)$. This model resembles the one discussed in the first section and the one studied in Khadra et al. (2003a). In this new model, system (22) is impulsively driven by system (21), using the matrices B_i, $i = 1, 2, \ldots$, and continuously driven by the signal $\mathbf{\Phi}(\mathbf{x}(t-\widetilde{r}))$, where $\widetilde{r}$ represents the transmission delay. The solution trajectories of system (21) in the state spaces (x_1, x_2, x_3), (x_1, x_2, x_4), (x_1, x_3, x_4) and (x_2, x_3, x_4), are displayed in Figs. 3(a), (c), (e) and (g), respectively, whereas the trajectories of the system (22) in the state spaces (u_1, u_2, u_3), (u_1, u_2, u_4), (u_1, u_3, u_4) and (u_2, u_3, u_4), are shown in Fig. 3(b), (d), (f) and (h), respectively. In addition, the time evolution of the state variables of both systems (21) and (22) are shown in Fig. 4(a) and (b), respectively, where the first component of each system is represented by a solid curve, the second component by a dashed curve, the third component by a dashed–dotted curve and the fourth component by a dotted curve. Notice their identical behaviour, although they start from different initial

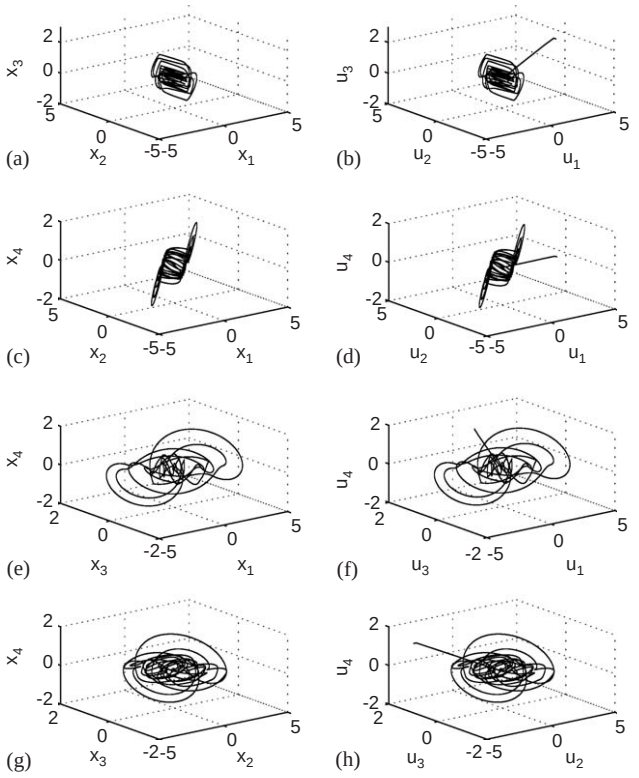

Fig. 3. Solution trajectories of systems (21) and (22) in the state spaces (a) (x_1, x_2, x_3), (b) (u_1, u_2, u_3), (c) (x_1, x_2, x_4), (d) (u_1, u_2, u_4), (e) (x_1, x_3, x_4), (f) (u_1, u_3, u_4), (g) (x_2, x_3, x_4), (h) (u_2, u_3, u_4).

conditions. The identical behaviour is verified by considering the error system, given by

$$\left\{\begin{array}{l} \dot{\mathbf{e}}(t)=\boldsymbol{\Psi}_1(\mathbf{x}(t),\mathbf{u}(t)) \\ \qquad +\boldsymbol{\Psi}_1(\mathbf{x}(t-\widetilde{r}),\mathbf{u}(t-\widetilde{r})) \\ \qquad +A\mathbf{e}(t)+\boldsymbol{\Psi}_2(\mathbf{x}(t),\mathbf{u}(t)), \quad t\neq\tau_i, \\ \Delta\mathbf{e}(t)=B_i\mathbf{e}(t-r_i), \quad t=\tau_i \ i=1,2,\ldots, \\ \mathbf{e}(t)=\boldsymbol{\phi}(t-t_0), \quad t_0-r\leqslant t\leqslant t_0, \end{array}\right\} \quad t>t_0, \tag{23}$$

where, $\boldsymbol{\Psi}_1(\mathbf{x},\mathbf{u})=\boldsymbol{\Phi}_1(\mathbf{x})-\boldsymbol{\Phi}_1(\mathbf{u})$, $\boldsymbol{\Psi}_2(\mathbf{x},\mathbf{u})=\boldsymbol{\Phi}_2(\mathbf{x})-\boldsymbol{\Phi}_2(\mathbf{u})$, $\boldsymbol{\phi}(t-t_0)$ is an initial constant function and $r=\max_i\{r_i,\widetilde{r}\}$. Theorem 4 gives the sufficient conditions under which the error system (23) is equi-attractive in the large, i.e., $\mathbf{e}\to\mathbf{0}$, as $t\to 0$.

Notice that

$$\begin{aligned}\|\boldsymbol{\Psi}_1(\mathbf{x},\mathbf{u})\| &= \|\boldsymbol{\Phi}_1(\mathbf{x})-\boldsymbol{\Phi}_1(\mathbf{u})\| \\ &= 20|g(x_2-x_1)-g(x_2-x_1)| \\ &\leqslant 124(|e_2|+|e_1|)\leqslant 124\|\mathbf{e}\|.\end{aligned}$$

Similarly, it can be checked that $\|\boldsymbol{\Psi}_2(\mathbf{x},\underline{\mathbf{u}})\|\leqslant 24.8\|\mathbf{e}\|$. With the above model, we have $\|A\|=20$, $2\widetilde{\lambda}=18.5$, $L_1=248$, $L_2=24.8$ and $a=282.05$. Thus, by applying equi-distant stabilizing impulses with $\Delta_i=\Delta=0.002$ and $B_i=B=-I$, for all $i=1,2,\ldots$, where I is the identity matrix, we obtain

$$\mathscr{K}_i=\mathscr{K}=\exp[a\Delta+L_1\Delta e^{a\delta}]=1.9180,$$

$$\begin{aligned}\mathscr{L}_i &= \mathscr{L} \\ &= \exp\left[a(k+\widetilde{k})\Delta+\frac{L_1}{a}e^{(k+\widetilde{k})a\Delta}-\frac{L_1}{a}\right] \\ &= \exp[0.5641(k+\widetilde{k})+0.0879e^{0.5641(k+\widetilde{k})}-0.0879].\end{aligned}$$

Therefore, according to Theorem 4 and Remark 1, system (23) is equi-attractive in the large if $r_i\mathscr{L}[\|A\|+2L_1+L_2]<\gamma^{k_i+\widetilde{k}}$, for all $i=1,2,\ldots$. It follows that the maximum delay which the error system can endure in the impulses, is given by

$$\begin{aligned}r_i<r_{\max}&=1.8491\times10^{-3} \\ &\quad\times\exp[0.0879(1-e^{0.5641(k+\widetilde{k})})-0.5641(k+\widetilde{k})]\end{aligned}$$

for all $i=1,2,\ldots$ and for $\gamma\approx 1$. Notice that $r_{\max}$, in this case, is smaller than 0.002. This implies that $k=1$, for all

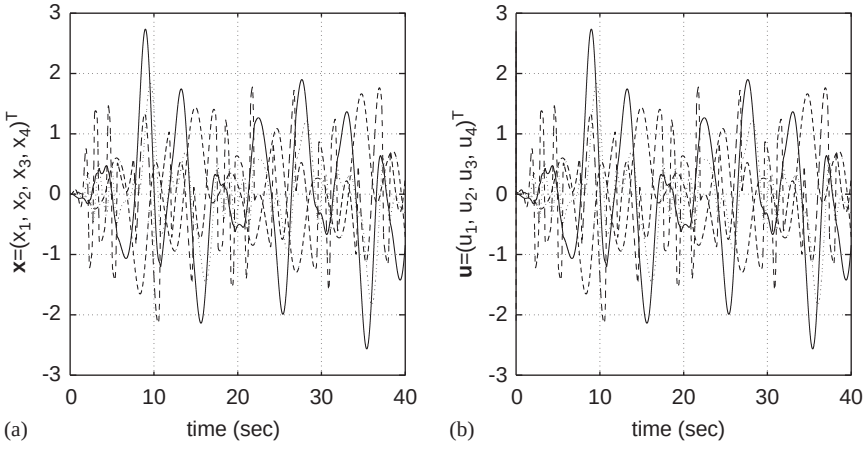

Fig. 4. Time evolution of the state variables for (a) system (21); (b) system (22).

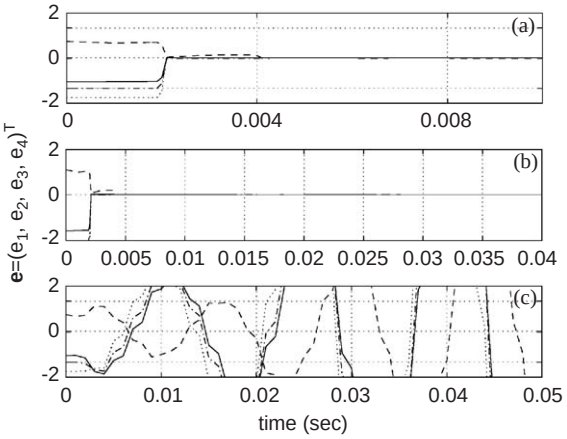

Fig. 5. Solution trajectories of system (23) with the presence of delay. (a) $\widetilde{r}=0.001$ and $\overline{r}=0.0004$; (b) $\widetilde{r}=0.001$ and $\overline{r}=0.001$. (c) $\widetilde{r}=1$ and $\overline{r}=0.0021$.

$i=1,2,\ldots$. Hence

$$r_i < r_{\max} = 1.8491\times 10^{-3}\exp[0.0879(1-\mathrm{e}^{0.5641(1+\widetilde{k})}) - 0.5641(1+\widetilde{k})] \tag{24}$$

for $i=1,2,\ldots$. From (24), we may conclude that as $\widetilde{r}\to\infty$, $\widetilde{k}\to\infty$ and $r_{\max}\to 0$, which reflects the nature of the relationship between the two delay terms. In general, it can be checked that as $\widetilde{r}$ increases, the upper bound on r_i, for all $i=1,2,\ldots$, given by $r_{\max}$, decreases.

If the delay term $\widetilde{r}=0.001$, then $\widetilde{k}=1$. It follows that

$$r_{\max}=0.4979\times 10^{-3}.$$

This means that if the delay terms r_i, for all $i=1,2,\ldots$, are all bounded above by $r_{\max}$, then Theorem 4 will guarantee that system (23) remains equi-attractive in the large. This is reflected in the numerical simulations, employing the Runge–Kutta method, presented in Fig. 5(a), where the initial constant function is given by $\boldsymbol{\phi}(t-t_0)=\boldsymbol{\phi}(t)=(1.12,-1,0.5,-0.2)^{\mathrm{T}}$ ($t_0=0$), the integration step-size is taken to be 0.0001 and the delay terms to be $\widetilde{r}=0.001$ and $r_i=\overline{r}=0.0004$, for all $i=1,2,\ldots$. It can be seen that the solution curves, presented by a solid curve for $e_1(t)$, dashed curve for $e_2(t)$, dashed–dotted curve for $e_3(t)$ and dotted curve for $e_4(t)$, all converge to zero. In addition, Fig. 5(b) shows that the desired result of equi-attractivity in the large is still achieved, although $\widetilde{r}=0.001$ and $r_i=\overline{r}=0.001>r_{\max}$, for all $i=1,2,\ldots$, which indicates that the conditions of Theorem 4 are sufficient conditions but not necessary, as discussed in Remark 4. Finally, taking the delay term $\widetilde{r}=1$ and $r_i=\overline{r}=0.0021$, for all $i=1,2,\ldots$, the synchronization is lost and the equi-attractivity in the large of system (23) fails, as shown in Fig. 5(c). Actually, without the presence of the delay term $\widetilde{r}$, i.e., when $\widetilde{r}=0$, and keeping $\overline{r}=0.0021$, the numerical simulation shows that system (23) remains equi-attractive in the large, as shown in Fig. 6. This kind of relationship between $\widetilde{r}$ and $r_{\max}$ is already expected in view of Eq. (24) and Remark 3.

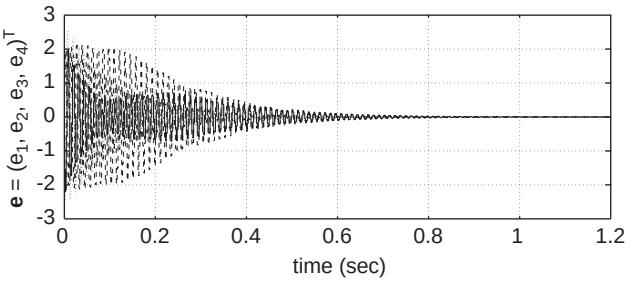

Fig. 6. Solution trajectories of system (23) with $\widetilde{r}=0$ and $\overline{r}=0.0021$.

5. Cryptosystem based on hyperchaos

In this section, we shall construct a cryptosystem similar to the one presented in Khadra et al. (2003a). However, in the upcoming model, the chaotic signals are generated by hyperchaotic systems installed at the transmitter and at the receiver ends. In addition, the applications of Theorem 4 and Corollary 5 to this hyperchaos-based communication security system will be investigated.

The proposed cryptosystem is shown in Fig. 7, where two hyperchaotic systems $\mathbf{x}$ and $\mathbf{u}$, which are used to mask-modulate and unmask the message signal $m(t)$, respectively, are included. The hyperchaotic system $\mathbf{x}=(x_1,x_2,x_3,x_4)^{\mathrm{T}}$ is at the transmitter end, whereas the hyperchaotic system $\mathbf{u}=(u_1,u_2,u_3,u_4)^{\mathrm{T}}$ is at the receiver end. Let $m(t)$ be the information signal to be encrypted. The masking-modulating process of $m(t)$ is done through two operations: multiplication and addition, viz. $f(t):=e(m(t))=(-60x_2(t)m(t))+20[3x_1+1.6(|x_2-x_1+1|-|x_2-x_1-1|)]$, where $f(t)$ is the encrypted signal that will be used to drive the hyperchaotic system $\mathbf{u}$ at the receiver end. $s(t)$ is the transmitted signal. It consists of a sequence of time frames of length T. Each time frame is divided into two regions: synchronizing-impulses region of length Q, where the impulses are loaded, and the encryption region of length $T-Q$, where $f(t)$ is loaded. The two regions are combined at the transmitter and then sent across a public channel to the receiver. At the receiver, each time frame of $s(t)$ is decomposed into the encrypted message $f(t)$ and the synchronizing impulses. At this point, $f(t)$ is used to drive the system $\mathbf{u}$, whereas the impulses are used to impulsively synchronize $\mathbf{u}$ with $\mathbf{x}$. When

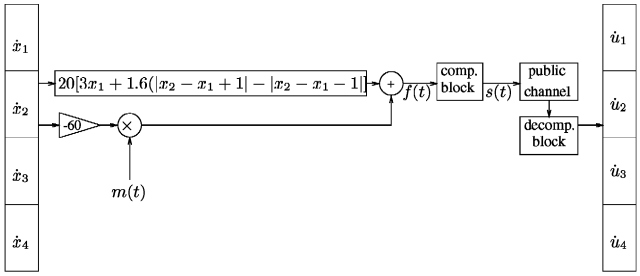

Fig. 7. Encryption process of $m(t)$.

Table 1
Binary representation of the English alphabet

Letter	Value	Binary	Letter	Value	Binary
A	10	001010	*N*	23	010111
B	11	001011	*O*	24	011000
C	12	001100	*P*	25	011001
D	13	001101	*Q*	26	011010
E	14	001110	*R*	27	011011
F	15	001111	*S*	28	011100
G	16	010000	*T*	29	011101
H	17	010001	*U*	30	011110
I	18	010010	*V*	31	011111
J	19	010011	*W*	32	100000
K	20	010100	*X*	33	100001
L	21	010101	*Y*	34	100010
M	22	010110	*Z*	35	100011

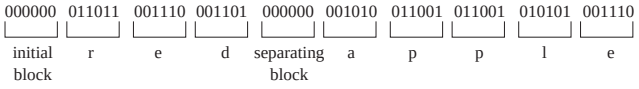

Fig. 8. Binary representation of the text “red apple”.

synchronization is achieved, we have $\mathbf{x} \approx \mathbf{u}$. Thus the decryption process of $f(t)$ becomes feasible by applying the operation

$$m(t) \approx \widehat{m}(t) = d(f(t)) = \frac{f(t) - 20[3u_1 + 1.6(|u_2 - u_1 - 1| - |u_2 - u_1 + 1|)]}{-60u_2}.$$

We shall present a numerical example involving the above scheme and using the plain text “red apple”. The basic idea of generating a signal $m(t)$ representing any plain text is to assign numbers to the English alphabet. For the letter ‘*A*’, we assign the number 10, for the letter ‘*B*’, we assign the number 11, and so on till we reach the last letter ‘*Z*’ whose assigned value is 35, as shown in Table 1. These numbers are transferred to their binary representation (with appropriate number of zeros added to the left to make all of them six-digit numbers) and a piecewise continuous signal $m(t)$ consisting of a sequence of step functions is generated to reflect these binary representations of any plain text. The way the signal $m(t)$ is constructed is done by forming a sequence of steps and blocks. Each block consists of 6 steps, where each step has length 0.05 s and height (or magnitude) equal to 0 or 1 depending on the value of the binary digit in the binary representation of the plain text. Each block represents the binary representation of one English letter only, as shown in Table 1. The signal $m(t)$ becomes complete when it is preceded by a block of 0s (i.e., the first block of $m(t)$ is a set of six steps of magnitude 0), in order to avoid the transient region (TR) of impulsive synchronization, and the words are separated by blocks of 0s. Using the above set up, the binary representation of the plain text “red apple” becomes the sequence shown in Fig. 8 and the piecewise continuous signal $m(t)$ representing this plain text is shown in Fig. 9 (a). Certainly, implementing the cryptosystem described earlier, there will be two types of delay involved in the system. Delay in the impulses, denoted by r_i, for all $i = 1, 2, \ldots$, and in the differential system, denoted by $\widetilde{r}$, identical to those discussed in the previous sections. We shall concern ourselves, however, in this numerical set up with the first type of delay r_i. i.e., we shall assume that the transmission delay is zero and we just have sampling delay. For an accurate decryption of the signal $f(t)$, identical synchronization between the two hyperchaotic systems, at the transmitter and receiver ends, is required. Now choosing the matrices B_i, to be $-I$, where I is the identity matrix, the delay terms $r_i = 0.0008$ ($\widetilde{k} = 0$) and $\Delta_i = 0.002$, for all $i = 1, 2, \ldots$, and using the Runge–Kutta method of step-size 0.0001 for integration, the numerical simulation of the error dynamics **e** shows identical synchronization starting from time 0.004 s, as expected from the discussion we had in the previous section (see Fig. 10). Furthermore, the simulation of $\widehat{m}(t)$ is identical to the graph of $m(t)$, as shown in Fig. 9(c), where Fig. 9(b) shows the TR. This can be seen in Fig. 11 which shows the graph of $\widehat{m}(t) - m(t)$ decaying to zero as $t \to \infty$. When $\widehat{m}(t)$ is retrieved at the receiver end, transferring the signal into a plain text is done through the

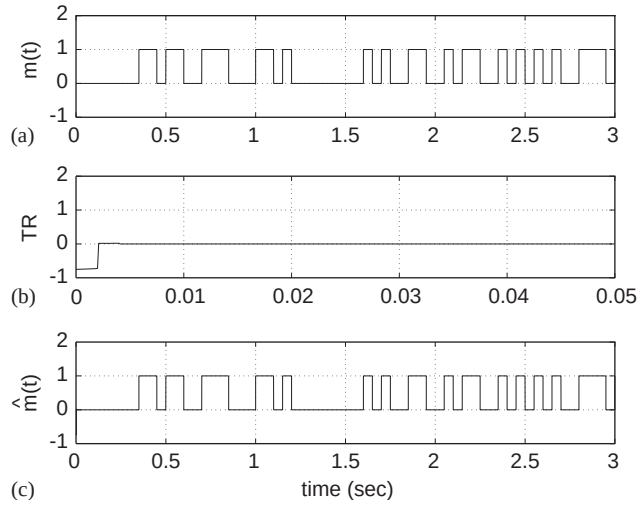

Fig. 9. (a) Original information signal $m(t)$. (b) Transient region (TR). (c) Decrypted signal $\widehat{m}(t)$.

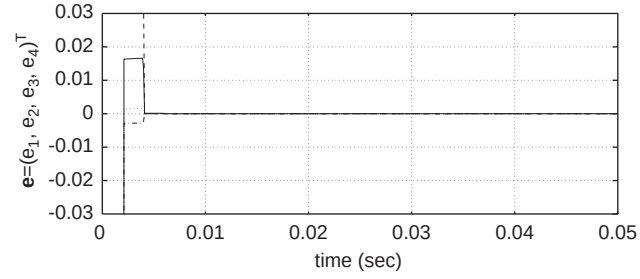

Fig. 10. Components of the error dynamics **e** approaching zero as $t \to \infty$.

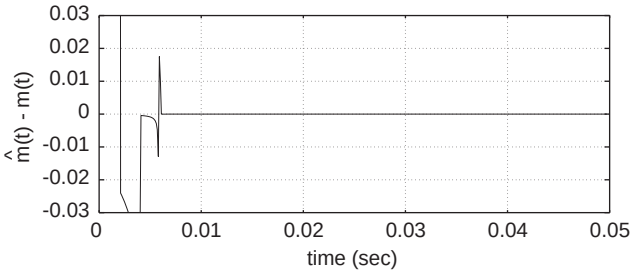

Fig. 11. The difference of $\widehat{m}(t) - m(t)$.

same procedure as the one to construct $m(t)$, i.e, by dividing the signal into blocks of six steps and reading the steps inside each block. The plain text "red apple" can therefore be recovered.

6. Conclusion

We have shown that the time delay in the impulsive differential system has direct impact on the upper bound of the delay in the impulses which the system can endure without losing its equi-attractivity property. Since delay in secure communication schemes is inevitable, the mathematical framework in this paper provides a suitable set of sufficient conditions to deal with such an issue, especially when dealing with communication schemes for impulsive and continuous driving between chaotic systems.

References

Amritkar, R. E., & Gupte, N. (1993). Synchronization of chaotic orbits: the effect of a finite time steps. *Physical Review E*, *47*(6), 3889–3895.

Ballinger, G. H., & Liu, X. Z. (1999). Existence and uniqueness results for impulsive delay differential equations. *Dynamics of Continuous, Discrete and Impulsive Systems*, *5*, 579–591.

Ballinger, G. H., & Liu, X. Z. (2000). Existence, uniqueness and boundedness results for impulsive delay differential equations. *Applicable Analysis*, *74*(1–2), 71–93.

Cuomo, K. M., & Oppenheim, A. (1993). Chaotic signals and systems for communications. *IEEE ICASSP*, *3*, 137–140.

Grassi, G., & Mascolo, S. (1997). Non-linear observer design to synchronize hyperchaotic systems via a scalar signal. *IEEE Transactions on Circuits and Systems-I*, *44*(10), 1011–1014.

Grassi, G., & Mascolo, S. (1999a). A system theory approach for designing cryptosystems based on hyperchaos. *IEEE Transactions on Circuits and Systems-I*, *46*(9), 1135–1138.

Grassi, G., & Mascolo, S. (1999b). Synchronizing hyperchaotic systems by observer design. *IEEE Transactions on Circuits and Systems-II*, *46*(4), 478–483.

Guan, Z. H., Chan, C. W., Leung, Y. T., & Chen, G. (2001). Robust stabilization of singular-impulsive-delayed systems with non-linear perturbations. *IEEE Transactions on Circuits and Systems-I*, *48*(8), 1011–1019.

Halle, K. S., Wu, C. W., Itoh, M., & Chua, L. O. (1993). Spread spectrum communication through modulation of chaos. *International Journal of Bifurcation and Chaos*, *3*(2), 469–477.

Itoh, M., Yamamoto, N., Yang, T., & Chua, L. O. (1999). Performance analysis of impulsive synchronization. *Proceedings of the 1999 european conference on circuit theory and design*, Stresa, Italy (pp. 353–356).

Itoh, M., Yang, T., & Chua, L. O. (1999). Experimental study of impulsive synchronization of chaotic and hyperchaotic circuits. *International Journal of Bifurcation and Chaos*, *9*(7), 1393–1424.

Itoh, M., Yang, T., & Chua, L. O. (2001). Conditions for impulsive synchronization of chaotic and hyperchaotic systems. *International Journal of Bifurcation and Chaos*, *11*(2), 551–560.

Khadra, A., Liu, X. Z., & Shen, X. (2003a). Robust impulsive synchronization and application to communication security. *Dynamics of Continuous, Discrete and Impulsive Systems, Series B: Applications & Algorithms*, *10*, 403–416.

Khadra, A., Liu, X. Z., & Shen, X. (2003b). Application of impulsive synchronization to communication security. *IEEE Transactions on Circuits and Systems-I*, *50*(3), 341–351.

Kocarev, L., Halle, K. S., Eckert, K., Chua, L. O., & Parlitz, U. (1992). Experimental demonstration of secure communications via chaotic synchronization. *International Journal of Bifurcation and Chaos*, *2*(3), 709–713.

Lakshmikantham, V., & Liu, X. Z. (1993). *Stability analysis in terms of two measures*. Singapore: World Scientific.

Li, Z. G., Wen, C. Y., & Soh, Y. C. (2001). Analysis and design of impulsive control systems. *IEEE Transactions on Automatic Control*, *46*, 894–899.

Li, Z. G., Wen, C. Y., Soh, Y. C., & Xie, W. X. (2001). The stabilization and synchronization of Chua's oscillators via impulsive control. *IEEE Transactions on Circuits and Systems-I*, *48*(11), 1351–1355.

Matsumoto, T., Chua, L. O., & Kobayashi, K. (1986). Hyperchaos: laboratory experiment and numerical confirmation. *IEEE Transactions on Circuits and Systems-I*, *33*(11), 1143–1147.

Pecora, L., & Carroll, T. (1990). Synchronization in chaotic systems. *Physical Review Letters*, *64*(8), 821–824.

Peng, J. H., Ding, E. J., Ding, M., & Yang, W. (1996). Synchronizing hyperchaos with scalar transmitted signal. *Physical Review Letters*, *76*(6), 904–907.

Stojanovski, T., Kocarev, L., & Parlitz, U. (1996). Driving and synchronizing by chaotic impulses. *Physical Review E*, *43*(9), 782–785.

Suykens, J. A., Yang, T., & Chua, L. O. (1998). Impulsive synchronization of chaotic Lur'e systems by measurement feedback. *International Journal of Bifurcation and Chaos*, *8*(6), 1371–1381.

Yang, T., & Chua, L. O. (1997a). Impulsive stabilization for control and synchronization of chaotic systems: theory and application to secure communication. *IEEE Transactions on Circuits and Systems-I*, *44*(10), 976–988.

Yang, T., & Chua, L. O. (1997b). Impulsive control and synchronization of non-linear dynamical systems and application to secure communication. *International Journal of Bifurcation and Chaos*, *7*(3), 645–664.

Yang, T., & Chua, L. O. (1999). Generalized synchronization of chaos via linear transformations. *International Journal of Bifurcation and Chaos*, *9*(1), 215–219.

Anmar Khadra received the B.Sc. degree in pure mathematics (honours) with distinction from Concordia University, Montreal, QC, Canada, in 1997, and the M.Math and Ph.D. degrees in applied mathematics and electrical engineering from the University of Waterloo, Waterloo, ON, Canada, in 1999 and 2004, respectively, where he has been a research fellow as well in 2004. He is currently a Post-Doctoral fellow in the Mathematics

Department at the University of British Columbia, Vancouver, Canada, since January 2005. His research interests are dynamical systems, neural networks and secure communication. In particular, his work focuses on stability theory, nonlinear oscillators, chaos, synchronization, impulsive systems and modelling.

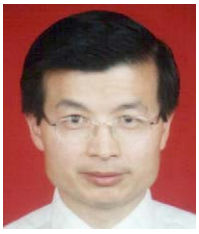

Xinzhi Liu received the B.Sc. degree in mathematics from Shandong Normal University, Jinan, China, in 1982, and the M.Sc. and Ph.D. degrees, all in applied mathematics, from University of Texas, Arlington, in 1987 and 1988, respectively. He was a Post-Doctoral Fellow at the University of Alberta, Edmonton, AB, Canada, from 1988 to 1990. He joined the Department of Applied Mathematics, University of Waterloo, Waterloo, ON, Canada, in 1990, where he became an Associate Professor in 1994, and a Professor in 1997. His research areas include systems analysis, stability theory, hybrid dynamical systems, impulsive control, chaos synchronization, nonlinear oscillations, artificial neural networks, and communication security. He is the author or coauthor of over 150 research articles and two research monographs and five other books. He is the Chief Editor of the journal, *DCDIS Series A*: *Mathematical Analysis*, and the Chief Editor of the Journal, *DCDIS Series B*: *Applications and Algorithms*, and Associate Editor of four other journals. Dr. Liu served as General Chair for several international scientific conferences.

Xuemin (Sherman) Shen received the B.Sc. (1982) degree from Dalian Maritime University (China) and the M.Sc. (1987) and Ph.D. degrees (1990) from Rutgers University, New Jersey (USA), all in electrical engineering. From September 1990 to September 1993, he was first with the Howard University, Washington DC, and then the University of Alberta, Edmonton (Canada). Since October 1993, he has been with the Department of Electrical and Computer Engineering, University of Waterloo, Canada, where he is a Professor. Dr. Shen's research focuses on mobility and resource management in interconnected wireless/wireline networks, UWB wireless communications, ad hoc networks, and sensor networks. He is a coauthor of two books, and has publications in communications networks, control and filtering. Dr. Shen serves as the Technical Co-Chair, IEEE Globecom'03 Symposium on Next Generation Networks and Internet; and ISPAN'04; the Editor, IEEE Trans. Wireless Communications, IEEE Trans. Vehicular Technology, and three other journals; Guest Editor, IEEE JSAC—Special Issue on Ultra Wideband Wireless Communications; IEEE Communications Magazine—Special Issue on China Wireless Communications: Technology vs. Markets; IEEE Wireless Communications—Special Issue on 4G Mobile Communication—Towards Open Wireless Architecture. Dr. Shen received the Premier's Research Excellence Award (PREA) from the Province of Ontario for demonstrated excellence of scientific and academic contributions, and the Distinguished Performance Award from the Faculty of Engineering, University of Waterloo, for outstanding contribution in teaching, scholarship and service. Dr. Shen is a senior member of the IEEE, and a registered Professional Engineer of Ontario, Canada.